# Comparison of the Photochemistry of 3-Methyl-2-phenyl-2*H*-azirine and 2-Methyl-3-phenyl-2*H*-azirine

Xiaoming Zhang, Sujan K. Sarkar, Geethika K. Weragoda, Sridhar Rajam, Bruce S. Ault, and Anna D. Gudmundsdottir*

Department of Chemistry, University of Cincinnati, Cincinnati, Ohio 45221-0172, United States

S *Supporting Information*

ABSTRACT: Photolysis of 3-methyl-2-phenyl-2*H*-azirine (**1a**) in argon-saturated acetonitrile does not yield any new products, whereas photolysis in oxygen-saturated acetonitrile yields benzaldehyde (**2**) by interception of vinylnitrene **5** with oxygen. Similarly, photolysis of **1a** in the presence of bromoform allows the trapping of vinylnitrene **5**, leading to the formation of 1-bromo-1-phenylpropan-2-one (**4**). Laser flash photolysis of **1a** in argon-saturated acetonitrile ($\lambda = 308$ nm) results in a transient absorption with λ_{max} at ~440 nm due to the formation of triplet vinylnitrene **5.** Likewise, irradiation of **1a** in cryogenic argon matrixes through a Pyrex filter results in the formation of ketene imine **11**, presumably through vinylnitrene **5**. In contrast, photolysis of 2-methyl-3-phenyl-2*H*-azirine (**1b**) in acetonitrile yields heterocycles **6** and **7**. Laser flash photolysis of **1b** in acetonitrile shows a transient absorption with a maximum at 320 nm due to the formation of ylide **8**, which has a lifetime on the order of several milliseconds. Similarly, photolysis of **1b** in cryogenic argon matrixes results in ylide **8**. Density functional theory calculations were performed to support the proposed mechanism for the photoreactivity of **1a** and **1b** and to aid in the characterization of the intermediates formed upon irradiation.
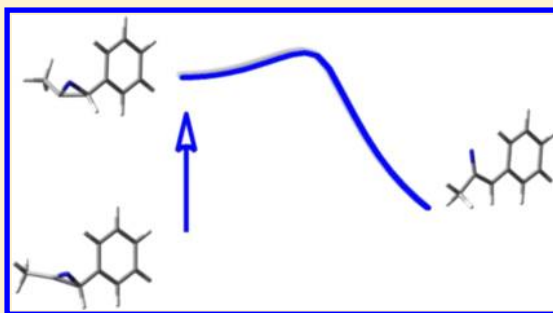
1. INTRODUCTION

Triplet nitrenes are electron-deficient reactive intermediates.[1] Electron-donating groups such as alkyl and aryl substituents render the triplet nitrenes more stable, and thus, they do not react with the solvent but rather decay by dimerization.[2−7] In contrast, electron-withdrawing groups destabilize nitrenes, making them more reactive. For example, triplet ester nitrenes react efficiently by abstracting a H atom from the solvent.[8−10] Interestingly, triplet vinylnitrenes that are stabilized by an electron-donating vinyl substituent react differently from alkyl- and arylnitrenes, as they decay by intersystem crossing.[11−13]

Solution photolysis of azirine derivatives can lead to the formation of triplet vinylnitrenes by breaking the C−N bond in the azirine.[13,14] Simple vinylnitrenes must decay by intersystem crossing to reform their starting materials as no new photoproducts were observed,[15,16] thus giving the impression that azirine derivatives are not photoreactive, whereas vinyl-nitrenes that have a carbonyl group at the γ-position can form isoxazole products in addition to reforming the starting material (Scheme 1).[11−14,17] However, triplet vinylnitrenes have been trapped with oxygen to form stable products in both solution and cryogenic matrixes.[11,15,16] Furthermore, the rate constant for the reaction of vinylnitrenes with oxygen in solution has been estimated to be between 7×10^8 and 2×10^9 M^{-1} s^{-1}.[11,13] Because of the significant 1,3-biradical character of vinyl-nitrenes, they react efficiently with oxygen to form a new C−O bond, whereas phenyl- and alkylnitrenes react with oxygen at a lower rate to form the corresponding nitro compounds.[3,5,18,19]

Scheme 1

Ar = p-NO$_2$Ph, Naphthalene
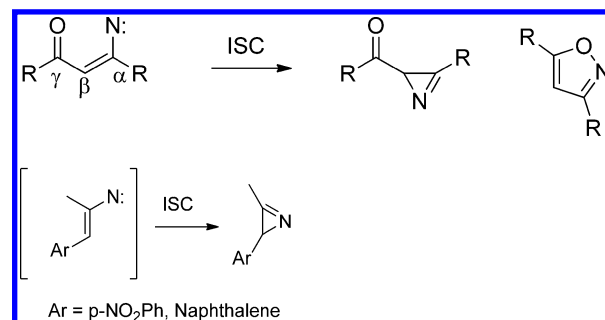
Photolysis of azirine derivatives can also lead to ylide formation by breaking the C−C bond of the azirine moiety (Scheme 2).[20−22] The ylide formation takes place on the singlet surface of the azirine, and the ylides are long-lived intermediates that can be trapped in 1,3-dipolar additions.[23,24]

In this work, we compared the photoreactivity of two 2*H*-azirine isomers to gain better insight into when the azirine

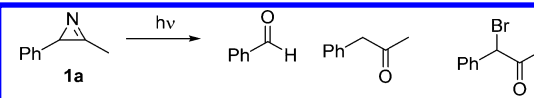**Scheme 2**
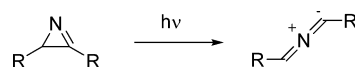
derivatives exhibit singlet versus triplet reactivity. We showed that upon irradiation with light above 300 nm, 3-methyl-2-phenyl-2H-azirine (**1a**) forms triplet vinylnitrene intermediate **5**, which can be detected directly with transient spectroscopy. Furthermore, in solution the triplet vinylnitrene **5** reforms **1a** but can be intercepted with oxygen and bromine radicals. In contrast, photolysis of 2-methyl-3-phenyl-2H-azirine (**1b**) results only in singlet reactivity to yield ylide **8**, and no formation of triplet vinylnitrene **10** was observed.

2. RESULTS

2.1. Product Studies. Photolysis of **1a** through a Pyrex filter in argon-saturated acetonitrile did not yield any new photoproducts. In contrast, the photolysis of **1a** in argon-saturated bromoform resulted in the formation of ketones **4**. Photolysis of **1a** in oxygen-saturated acetonitrile resulted in the formation of benzaldehyde (**2**), and irradiation of **1a** in oxygen-saturated bromoform yielded **2**, **3**, and **4** (Scheme 3).

Scheme 3

Product		2	3	4
Solvent				
CH$_3$CN	Ar			
	O$_2$	100		
CHBr$_3$	Ar			100
	O$_2$	10	9	81

We theorize that the irradiation of **1a** through a Pyrex filter yields triplet vinylnitrene **5**, which undergoes intersystem crossing to reform **1a**, but in the presence of oxygen, triplet vinylnitrene **5** is trapped to form **2** (Scheme 4). To better probe the reactivity of vinylnitrene **5**, we studied the photolysis
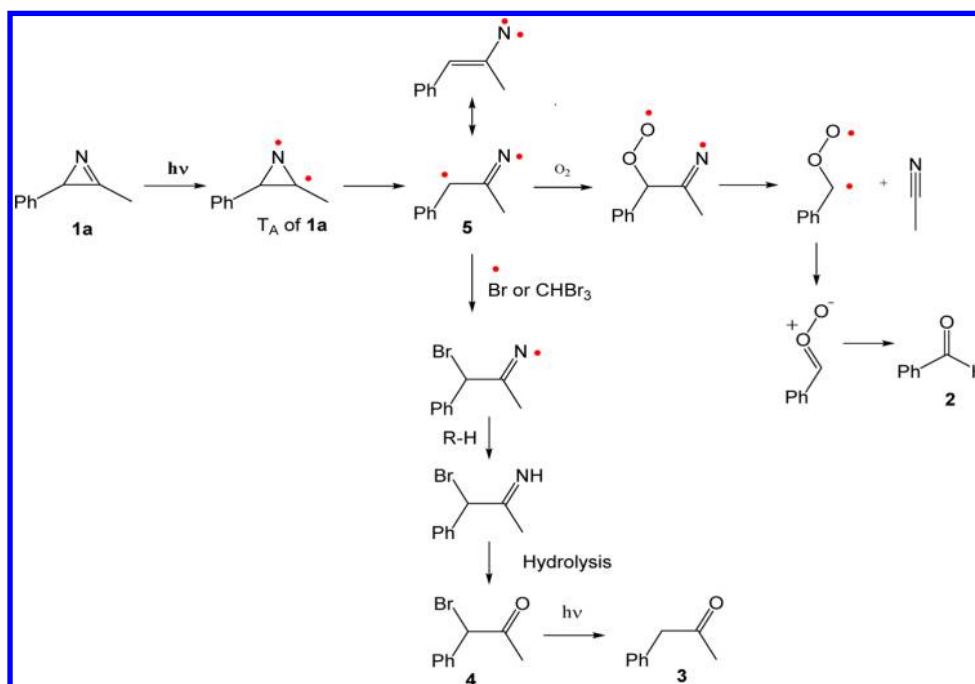
of **1a** in bromoform to determine whether vinylnitrene can be trapped by bromine radicals. It should be noted that direct irradiation of bromoform with light above 300 nm results in the quantitative formation of bromine radicals.[25] Because products **3** and **4** are formed only in bromoform, we theorize that the triplet vinylnitrene **5** is trapped with bromine radicals, as shown in Scheme 4, and that **3** is formed from the secondary photolysis of **4**. As expected, an independent photolysis of **4** through a Pyrex filter confirmed that **4** yields **3**. We also hypothesized that energy transfer from the excited state of **1a** to bromoform could result in the formation of bromine radicals in addition to direct photolysis of bromoform. Furthermore, we theorized that triplet vinylnitrene **5** can react directly with bromoform to abstract bromine atom to form **4** in addition to reacting with bromine radicals.

In contrast, the photolysis of **1b** in argon- and oxygen-saturated solutions through a Pyrex filter affords heterocycles **6** and **7** in a 1:3 ratio (Scheme 5). This is in agreement with the

Scheme 5
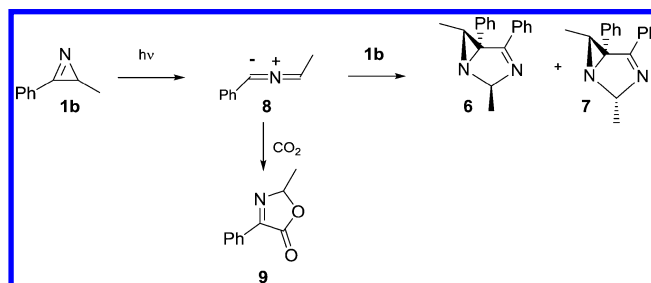
results obtained by Gakis et al.[24] and Padwa et al.,[26,27] who previously reported that the irradiation of **1b** results in **6** and **7**. These authors theorized that **6** and **7** are formed by trapping of ylide **8** in a 1,3-dipolar addition to **1b**. Furthermore, we also reconfirmed that ylide **8** can be trapped by a 1,3-dipolar

Scheme 4

addition to carbon dioxide to yield **9** by photolyzing **1b** in CO_2-saturated acetonitrile.[28−30]

Thus, the product studies indicate that the irradiation of **1a** through a Pyrex filter yields triplet vinylnitrene **5**, which can be intercepted with oxygen or bromine radicals, whereas the irradiation of **1b** yields products from singlet ylide **8**, which is trapped by bimolecular 1,3-dipolar cycloaddition reactions.

2.2. Calculations. To better understand why the reactivity of **1a** and **1b** differ and to better comprehend the reactivity of vinylnitrene **5** and ylide **8**, we calculated stationary points on the singlet and triplet energy surfaces of **1a** and **1b**. The calculations were performed using Gaussian09 at the B3LYP level of theory using the 6-31+G(d) basis set.[31−33]

We optimized the ground states (S_0) of **1a** and **1b** and used time-dependent density functional theory (TD-DFT) to estimate the vertical excitation energies of their first excited singlet states (S_1) and their first and second excited triplet states (T_1 and T_2). The S_1 are located at 106 kcal/mol (Figure 4) and 97 kcal/mol (Figure 5) above the corresponding S_0 for **1a** and **1b**, respectively. The T_1 of **1a** and **1b** are located at 83 and 70 kcal/mol and the T_2 at 96 and 87 kcal/mol above the corresponding S_0 states. Thus, the conjugation of the C=N bond with the phenyl ring in **1b** lowers the energies of S_1, T_1, and T_2 in **1b** in comparison to the energies of S_1, T_1, and T_2 in **1a**.

We optimized T_1 of **1a** and located it at 72 kcal/mol above its S_0, which is considerably lower than the energy for the Franck−Condon state described above (TD-DFT calculations). We have previously shown that the energy obtained from optimization of triplet ketones with an (n,π*) configuration is systematically underestimated by density functional theory,[34] but the difference in the energies for T_1 of **1a** obtained from the TD-DFT calculations and the optimization must be due to the geometrical difference in the optimized structures of T_1 and S_0 of **1a**. The most significant difference between the structures of T_1 and S_0 of **1a** is that the C=N bond length is 1.47 Å in the T_1 of **1a**, indicating that the bond is best described as a single bond (Figure 1). In addition, spin density calculations showed that the unpaired electrons are localized on the C and N atoms in the azirine moiety, thus demonstrating that the T_1 of **1a** is localized on the azirine moiety of the molecule (Figure 1).

The optimized structure of the T_1 of **1b** is 62 kcal/mol above its S_0, which is also considerably lower in energy than predicted from the TD-DFT calculations, and as before, the discrepancy must be due to geometrical differences between the T_1 and S_0 of **1b**. The most significant difference between the optimized structures of the T_1 of **1b** and its S_0 is the C=N bond, which has a length of 1.44 Å (Figure 1). Furthermore, the C−C bond between the azirine and the phenyl moiety is only 1.37 Å and thus somewhat shorter than in the S_0 of **1b**. In addition, the C−C bonds in the phenyl ring are not all equivalent. Thus, the T_1 of **1b** is delocalized over the phenyl and azirine moieties. Spin density calculations further support this, as the unpaired electron density is delocalized over both the phenyl and azirine moieties (Figure 1).

We optimized two minimal-energy conformers, A and B, of triplet vinylnitrene **5**, with A being 3 kcal/mol more stable than B. The Ph−C bond in vinylnitrene **5** is shorter than an average single C−C bond because the vinylnitrene moiety is in conjugation with the phenyl ring (Figure 2). This is further highlighted by the spin density calculations, which show that the unpaired electrons are mainly located on the N and β-C
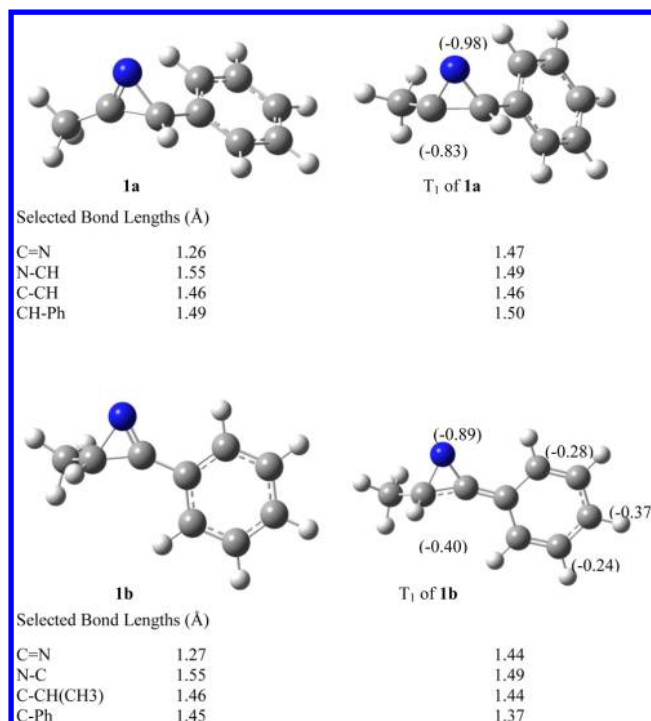

Figure 1. Optimized structures of **1a** and **1b**, the T_1 of **1a**, and the T_1 of **1b**. The numbers in parentheses are the calculated spin densities for the T_1 states of **1a** and **1b**.
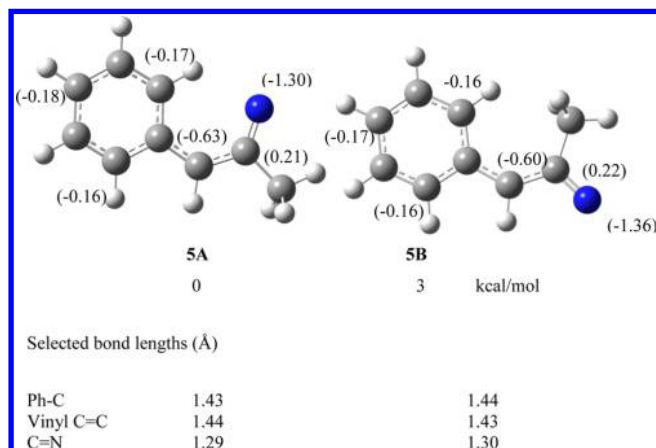

Figure 2. Optimized structures of conformers A and B of triplet vinylnitrene **5**. The numbers in parentheses are the calculated spin densities.

atoms in the vinylnitrene moiety and also on the *ortho* and *para* C atoms in the phenyl ring.

We also optimized two minimal energy conformers, A and B, of triplet vinylnitrene **10**, the nitrene that corresponds to azirine **1b** (Figure 3). Because the vinylnitrene moiety in **10** is in cross-conjugation with the phenyl ring, the spin density is mainly localized over the vinylnitrene moiety and not the phenyl group.

The transition state for the formation of triplet vinylnitrene **5** from the T_1 of **1a** is located 10 kcal/mol above the T_1 of **1a** (Figure 4). Thus, it is reasonable to expect that population of the T_1 of **1a** will result in the formation of triplet vinylnitrene **5**. As a comparison, the transition state barrier for forming vinylnitrene **10** from the T_1 of **1b** is 15 kcal/mol (Figure 5). Thus, the delocalization of the T_1 of **1b** over the entire
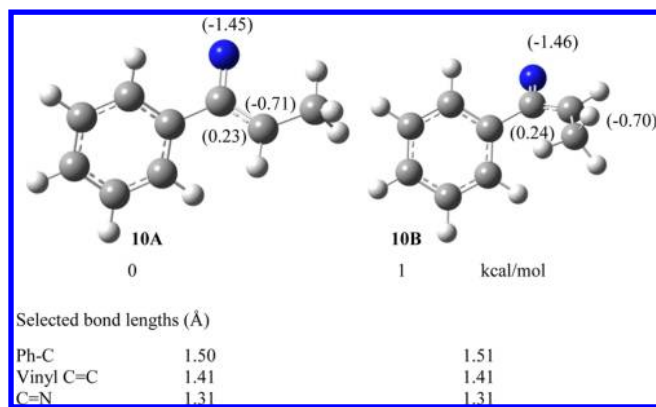
Figure 3. Optimized structures of conformers A and B of triplet vinylnitrene **10**. The numbers in parentheses are the calculated spin densities.
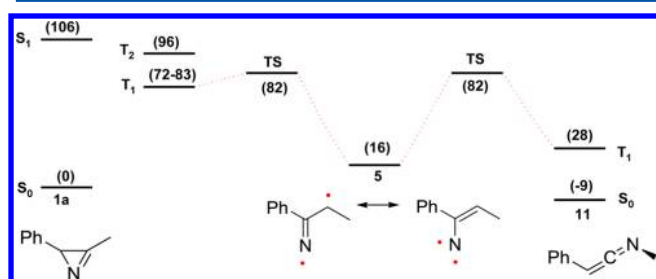

Figure 4. Calculated stationary points on the energy surface of **1a**. The numbers in parentheses are the calculated energies in kcal/mol. The energies of S_1 and T_2 and the value of 83 kcal/mol for T_1 were obtained by TD-DFT calculations, whereas the other energies were obtained by optimization calculations.
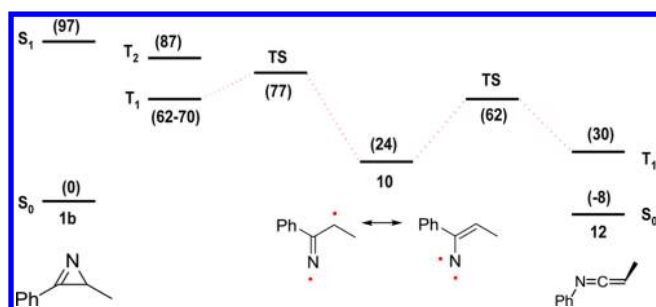

Figure 5. Calculated stationary points on the energy surface of **1b**. The numbers in parentheses are the calculated energies in kcal/mol. The energies of S_1 and T_2 and the value of 70 kcal/mol for T_1 were obtained by TD-DFT calculations, whereas the other energies were obtained by optimization calculations.

molecule stabilizes the T_1 of **1b**, which in turns makes it more difficult to break the N−C bond in the azirine ring to form vinylnitrene **10**.

We optimized the open-shell singlet vinylnitrenes **5** and **10** to estimate their triplet−singlet energy gaps and found that the energy gaps are 17 kcal/mol for **5** and 14 kcal/mol for **10** (Scheme 6). For comparison, we calculated the triplet−singlet energy gap for vinylnitrene ($CH_2=CH−N:$) and obtained a value of 16 kcal/mol, which is similar to the value of 15 kcal/mol reported by Parasuk and Cramer for vinylnitrene.[35] Although Wenthold and Hossain have demonstrated that radical stabilization by electron delocalization effectively reduces the triplet−singlet energy gap of vinylnitrenes,[36,37]

Scheme 6
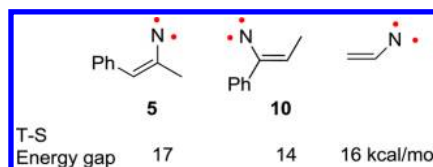
our calculations suggest that the phenyl group in **5** does not affect the triplet−singlet energy gap. In comparison, Nunes et al.[12] theorized that conical intersections between the triplet and open-shell singlet are responsible for effective intersystem crossing in vinylnitrene derivatives.

Because triplet vinylnitrenes typically undergo intersystem crossing to form ketene imines in cryogenic matrixes,[13,40−42] we calculated the triplet transition state for the formation of triplet ketene imine **11** from triplet vinylnitrene **5**. This transition state is located 66 kcal/mol above vinylnitrene **5**; in comparison, the transition state for the formation of triplet ketene imine **12** from triplet vinylnitrene **10** is 38 kcal/mol above **10**. Thus, the transition state barriers for triplet vinylnitrenes **5** and **10** to rearrange to the corresponding triplet ketene imines indicate that these rearrangements are not feasible. It is more likely that triplet vinylnitrenes **5** and **10** undergo intersystem crossing to form ketene imines **11** and **12**, respectively.

The calculated stationary points on the triplet surface for vinylnitrene **5** reacting with oxygen to form benzaldehyde **2** are displayed in Figure 6. Vinylnitrene **5** can react with oxygen to form biradical **13**, which is 8 kcal/mol more stable than **5** and O_2, and the calculated transition state barrier for this reaction is 6 kcal/mol above vinylnitrene **5** and O_2. Thus, the calculations show that vinylnitrene **5** is expected to react efficiently with molecular oxygen at ambient temperature. We theorized that biradical **13** can be cleaved to form biradical **14** and acetonitrile, but these products are 2 kcal/mol less stable than **13**, and the calculated transition state barrier for cleavage of **13** to form **14** and acetonitrile is 18 kcal/mol above **13**. Although **14** can undergo intersystem crossing to form ylide **15**, which is 27 kcal/mol more stable, it is more likely that biradical **13** forms ylide **15** via intersystem crossing, followed by hydrolysis to form benzaldehyde **2**. Thus, the calculations support the theory that triplet vinylnitrene **5** can react with oxygen at ambient temperature to form benzaldehyde **2**.

We calculated the feasibility of forming bromine radical from bromoform by energy transfer from the S_1 or T_1 of **1a** (Figure 7). The calculated bond dissociation energy for bromoform to form bromine radical is only 65 kcal/mol, significantly less than the energy of the S_1 and T_1 of **1a**. Thus, the calculations support the idea that **1a** can be used as a sensitizer to cleave bromoform to form bromine radicals. We could not calculate the transition state for the reaction of bromine radical with vinylnitrene **5** because of spin restrictions.

Addition of bromine radical to vinylnitrene **5** results in the formation of radical **16**, which is 56 kcal/mol more stable than **5** and bromine radical (Figure 7). Thus, the calculations show that the formation of bromine radical by sensitization and the addition of bromine radicals to vinylnitrene **5** are very feasible at ambient temperature.

In addition, we calculated the transition state barrier for the reaction of vinylnitrene **5** with bromoform to form **16** and $^\bullet CHBr_2$. The transition state barrier for **5** to abstract a bromine atom from bromoform to yield **16** and $^\bullet CHBr_2$ is 11 kcal/mol
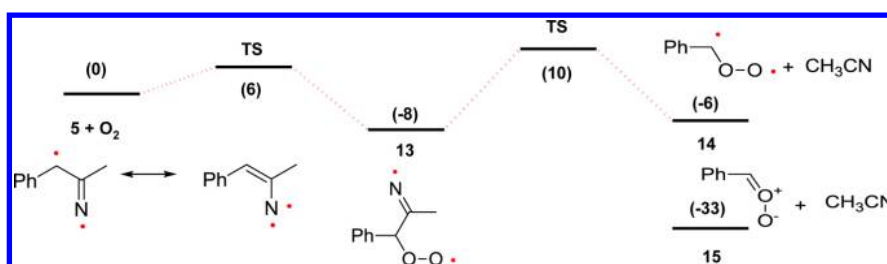
Figure 6. Calculated stationary points on the energy surface of triplet vinylnitrene **5** reacting with O₂. Energies are in kcal/mol.
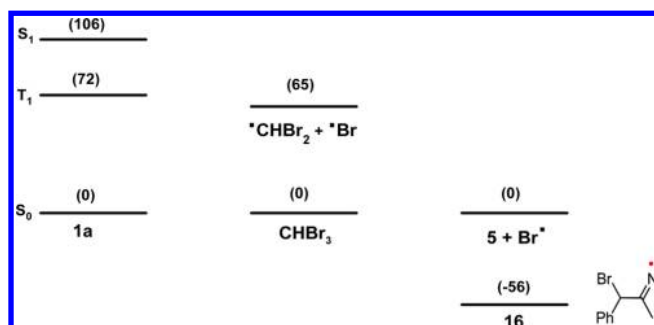

Figure 7. Energy calculation for the formation of bromine radicals from bromoform and trapping of vinylnitrene **5** with bromine radical. Energies are in kcal/mol.

Figure 9. Energy diagram for the formation of ylide **8** from **1b**.

(Figure 8). Thus, it is also possible for vinylnitrene **5** to abstract a bromine atom from bromoform directly.

Finally, we calculated the singlet reactivity of azirine **1b** to form ylide **8** (Figure 9). The transition state barrier for the formation of ylide **8** from azirine **1b** was located 43 kcal/mol above the S₀ of **1b**. The calculated transition state barrier for **1b** to form ylide **8** is similar to those we calculated for other azirine derivatives.[13]

2.3. Laser Flash Photolysis. To identify the intermediates formed upon the photolysis of **1a** and **1b**, we used laser flash photolysis (excimer laser, 17 ns, 308 nm). Laser flash photolysis of **1a** in argon-saturated acetonitrile produced a broad transient spectrum with λ_{max} at ~440 nm (Figure 10A). We assign this transient spectrum to triplet vinylnitrene **5** on the basis of the similarity between this transient spectrum and the calculated absorption spectrum of **5** (Figure 10B). The TD-DFT calculations in acetonitrile predicted the most significant electronic transitions above 300 nm for vinylnitrene **5A** at 301 nm (f = 0.070), 306 nm (f = 0.053), 405 nm (f = 0.0145), and 420 nm (f = 0.0104) and for vinylnitrene **5B** at 314 nm (f = 0.0155), 384 nm (f = 0.0027), and 398 nm (f = 0.0088). It should be emphasized that we could not measure the transient absorption below 330 nm because of the ground-state absorption of **1a**, and therefore could not verify that vinylnitrene **5** has a strong band at approximately 300 nm. In

Figure 10. (A) Transient UV−vis spectrum obtained by laser flash photolysis of **1a**. (B) Calculated absorption spectra of **5A**, **5B** and the T₁ of **1a** in acetonitrile. (C) Kinetic trace obtained at 460 nm.

comparison, the calculated spectrum of the T₁ of **1a** has its most significant electronic transitions at 303 nm (f = 0.0196), 304 nm (f = 0.0189), 342 nm (f = 0.0023), 391 nm (f = 0.0011), 480 nm (f = 0.0112), and 507 nm (f = 0.0008), which
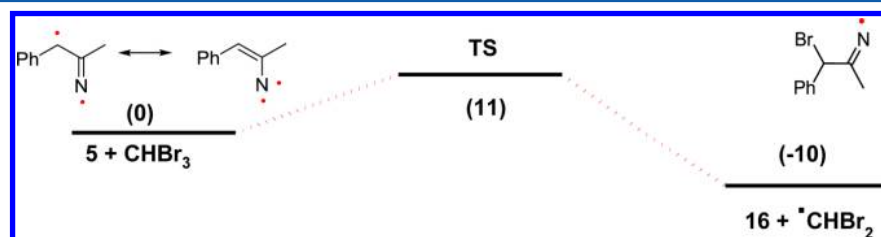
Figure 8. Energy diagram for the reaction of vinylnitrene **5** with bromoform to form **16** and •CHBr₂.

is a considerably broader absorption range than in the observed spectrum, thus further supporting the assignment of the transient to vinylnitrene **5**. The transient absorption was formed faster than the time resolution of the laser flash photolysis apparatus. The decay of the transient absorption at 460 nm (Figure 10C) was best fit as an exponential decay with a rate constant of 1.5×10^5 s^{-1}, corresponding to a lifetime of 7 μs. In oxygen-saturated solutions, the transient absorption was fully quenched, whereas in air-saturated methanol, the rate constant for the decay was 1.7×10^6 s^{-1}. The rate constant for quenching of triplet vinylnitrene with oxygen is 8.9×10^8 M^{-1} s^{-1} because the concentration of oxygen in air-saturated acetonitrile is 0.0019 M.[38] This rate constant for oxygen quenching is similar to those we have measured for different triplet vinylnitrene derivatives (7×10^8 and 2×10^9 M^{-1} s^{-1}).[11,13]

Laser flash photolysis of azirine **1b** in acetonitrile produced transient spectra with λ_{max} at ~320 nm (Figure 11A). We assign
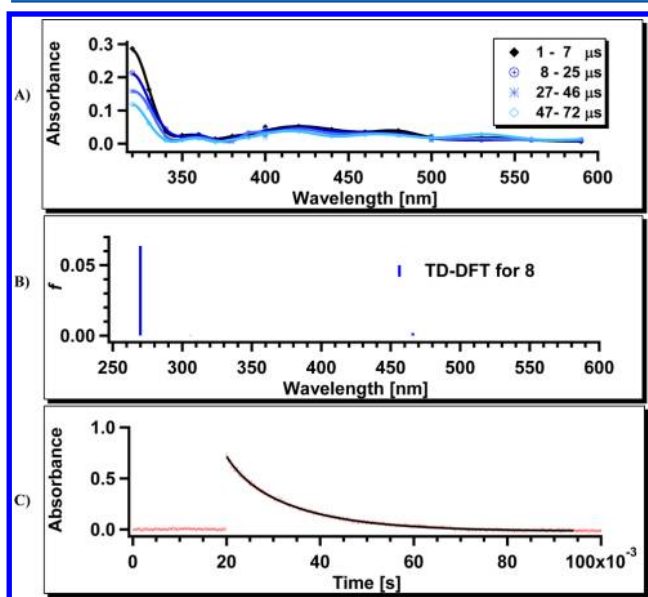

Figure 11. (A) Transient spectrum obtained by laser flash photolysis of **1b** in argon-saturated acetonitrile. (B) TD-DFT calculated spectrum for **8**. (C) Kinetic trace obtained at 320 nm.

the absorbance at 320 nm to ylide **8** on the following basis. Stenkeen and co-workers have shown previously that laser flash photolysis by 248 nm irradiation of 3-phenyl-2*H*-azirine derivatives yields ylides with λ_{max} at ~290 nm and a shoulder at ~400 nm.[23] Laser flash photolysis of **1b** with 308 nm irradiation does not allow detection of the transient absorption below 320 nm because of ground-state absorption of **1**, and thus, we observed only the tail absorption for ylide **8**. In addition, TD-DFT calculations showed that the major absorptions for **8** are placed at 270 nm ($f = 0.0636$), 306 nm ($f = 0.0002$) and 456 nm ($f = 0.0017$) (Figure 11B), which fits with the conclusion that we observed only the tail of the absorption of ylide **8**. The lifetime of ylide **8** at 320 nm is on the order of several milliseconds (Figure 11C). As expected, the transient spectrum of ylide **8** and its lifetime were not affected by oxygen.

Thus, the results of laser flash photolysis of **1a** and **1b** with a 308 nm laser are in agreement with the product studies performed by irradiation through Pyrex filter, as both sets of

experiments clearly demonstrate that **1a** exhibits triplet reactivity to form triplet vinylnitrene **5** whereas **1b** reacts on the singlet surface to form ylide **8**.

2.4. Stern–Volmer Analysis. To further characterize triplet vinylnitrene **5** and its reactivity, we analyzed how its formation and decay are affected by the addition of isoprene. Figure 12A shows the kinetic traces for triplet vinylnitrene **5** at
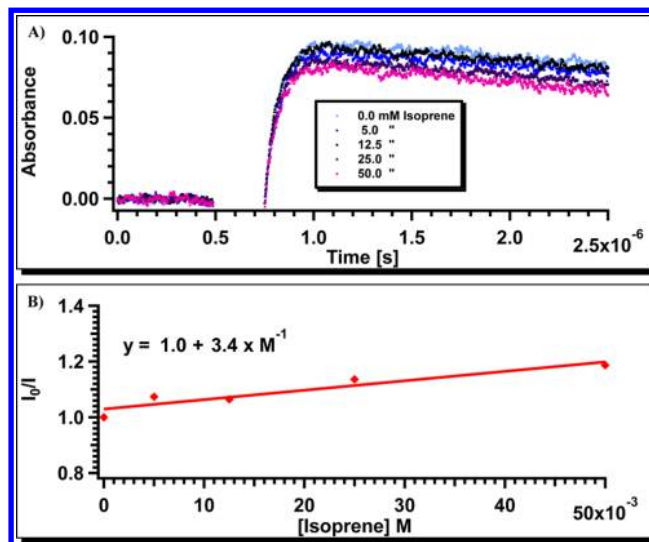

Figure 12. (A) Kinetic traces obtained at 460 nm from the laser flash photolysis of **1a** with various isoprene concentrations. (B) Stern–Volmer plot obtained from the kinetic traces shown in (A). I_0 is the absorption intensity in the absence of isoprene, and I is the absorption intensity at various isoprene concentrations.

460 nm with various amounts of isoprene. The intensity of the absorption was reduced upon the addition of isoprene, whereas the lifetime of **5** was not significantly affected, indicating that the isoprene quenches the precursor to vinylnitrene **5**. The Stern–Volmer plot yielded a straight line with a slope of 3.4 M^{-1} (Figure 12B). Thus, the lifetime of the precursor to triplet vinylnitrene **5** can be deduced as being between 3.4 and 0.34 ns by assuming that the quenching is diffusion-controlled (i.e., that k_q is between 10^9 and 10^{10} M^{-1} s^{-1}).

We also studied the effect of bromoform on the formation and decay of triplet vinylnitrene **5** in acetonitrile. The yield for the formation of vinylnitrene **5** decreased as the concentration of bromoform increased (Figure 13A), demonstrating that the precursor to vinylnitrene **5** is quenched with bromoform. A Stern–Volmer plot of I_0/I versus [bromoform] gave a slope of 2.1 M^{-1} (Figure 13B), and with the assumption that the quenching is diffusion-controlled, the precursor has a lifetime between 0.21 and 2.1 ns, which is the same lifetime, within experimental error, as obtained for the T$_1$ of **1a** by isoprene quenching. Hence, we conclude that T$_1$ of **1a** is quenched by bromoform to form bromine radicals. Addition of bromoform reduced not only the yield of vinylnitrene **5** but also its lifetime. Plotting the rate constant for the decay of vinylnitrene **5** as a function of the bromoform concentration yielded a straight line with a slope of 1.7×10^5 M^{-1}s^{-1} (Figure 13C). The reaction of vinylnitrene **5** with bromoform is significantly slower than that of vinylnitrene **5** with oxygen, which fits with the result that the transition state barrier for reaction of vinylnitrene **5** with bromoform (11 kcal/mol) is significantly larger than that for the reaction of vinylnitrene **5** with oxygen (6 kcal/mol).
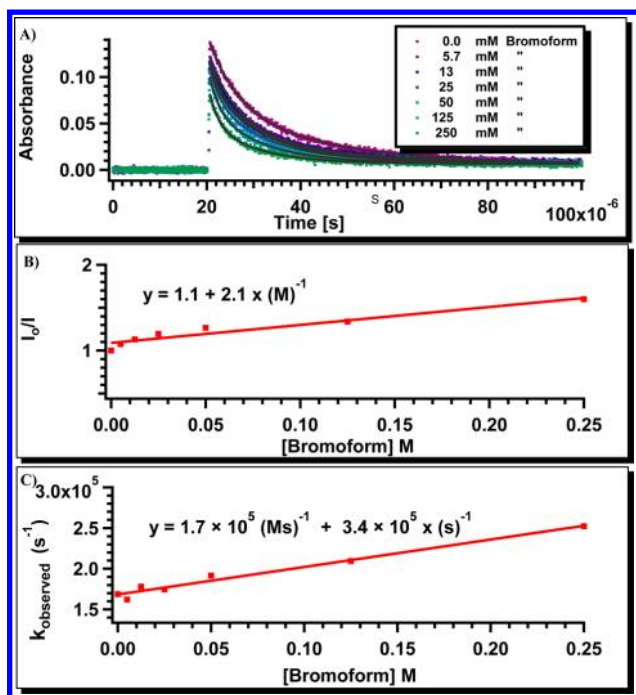
Figure 13. (A) Kinetic traces obtained at 460 nm from the laser flash photolysis of **1a** at various bromoform concentrations. (B) Stern–Volmer plot obtained from the kinetic traces shown in (A). I_0 is the absorption intensity in the absence of bromoform, and I is the absorption intensity at various bromoform concentrations. (C) The decay rate constant at 460 nm as a function of the bromoform concentration.

However, because bromine radicals are formed both by direct photolysis of bromoform and by sensitization of bromoform with **1a**, it is just as likely that vinylnitrene **5** reacts with bromine radicals rather than bromoform and that the lower rate is a reflection of the lower concentration of bromine radicals compared with bromoform.

2.5. Matrix Isolation. We studied the photolysis of **1a** and **1b** through a Pyrex filter in argon matrices at 14 K to confirm that **1a** and **1b** exhibit triplet and singlet reactivity, respectively. We deposited **1a** and **1b** into argon matrices in several different experiments, entraining the vapor over a sample of pure azirine in flowing argon and depositing the resulting sample on a 14 K cryogenic surface.

Photolysis of **1a** through a Pyrex filter for 2 h in argon matrices resulted in reductions of the IR bands at 1787, 1294, 1267, 1078, 1031, and 968 cm^{-1} (Figure 14). Concurrently, new bands were observed at 2054, 2043, 1071, 829, and 689 cm^{-1}. We assign these new bands to the formation of ketene
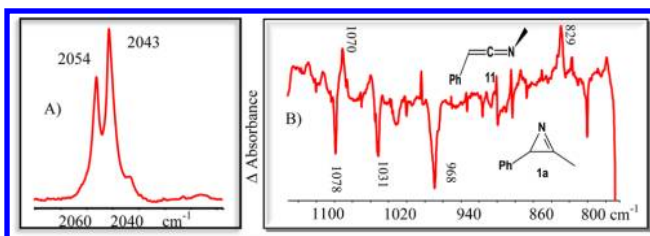

Figure 14. Matrix isolation spectra of **11**. (A) IR spectrum obtained after the photolysis of **1a** through a Pyrex filter. (B) Difference of the IR spectra of **1a** before and after irradiation through a Pyrex filter. The positive bands belong to **11** and the negative bands to **1a**.

imine **11** (Scheme 7) on the basis of the following observations. The calculated IR spectrum of **11** has an intense band at 2122

Scheme 7
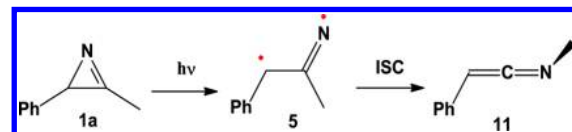
cm^{-1} ($f = 776$) due to C=C=N stretching, and scaling by 0.9613[39] places this band at 2040 cm^{-1}, which matches very closely with the observed bands at 2054 and 2043 cm^{-1}. The multiplet of this band is likely due to the presence of different conformers of **11**, which can also be trapped in different matrix sites. We assign the band at 1171 cm^{-1} to the stretch that is coupled between the phenyl ring and the C=C=N moiety, calculated to be at 1206 cm^{-1} ($f = 42$) or 1159 cm^{-1} with scaling. The band at 829 cm^{-1} is assigned to the coupled C=C=N and −CH$_3$ stretch at 903 cm^{-1} ($f = 14$), 868 cm^{-1} with scaling. Finally, we assign the band at 689 cm^{-1} to a coupled C=C=N and phenyl bending, which is calculated to be at 649 cm^{-1} ($f = 22$).

The photolysis of **1b** in argon matrices at 14 K resulted in the reduction or depletion of the bands at 1742, 1635, 1586, 1386, 1337, 1330, 1327, 1151, and 751 cm^{-1} (Figure 15). Concurrently, bands at 1895, 1887, 1859, 1374, 1292, 1263, 1137, 1069, 785, 783, 772, 770, 700, and 602 cm^{-1} were formed, and we assign them to ylide **8** (Scheme 8) on the basis of the following observations. The calculated IR spectrum of **8** has an intense band at 1968 cm^{-1} ($f = 133$) due to its C=N=C stretching. Scaling this band by 0.9613 places it at 1892 cm^{-1}, which fits nicely with the bands observed at 1895, 1887, and 1859 cm^{-1}. As before, we theorize that the multiplicity of this band is due to the presence of different conformers of **8**, which can also be trapped at different matrix sites. The band at 1374 cm^{-1} is assigned to wagging of the methyl group, which is calculated to be at 1426 cm^{-1} ($f = 16$); scaling places this band at 1371 cm^{-1}. The bands at 1292, 1263, and 1137 cm^{-1} are assigned to C−H wagging coupled with twisting of the aromatic ring and are calculated to be at 1336, 1303, and 1157 cm^{-1}. Furthermore, the band at 1069 cm^{-1} is assigned to twisting of the aromatic ring, which is calculated to be at 1103 cm^{-1} ($f = 23$). Finally, we assign the bands at 786 and 783 cm^{-1} to a coupled phenyl and C=N bending, calculated to be at 800 cm^{-1} ($f = 39$). The bands at 772, 770, and 700 cm^{-1} are assigned to N=C−H bending coupled to aromatic C−H bending, calculated to be at 788 cm^{-1} ($f = 31$) and 721 cm^{-1} ($f = 71$). Finally, we also observed C=N=C bending at 602 cm^{-1}, calculated to be at 620 cm^{-1} ($f = 88$).

Thus, the photolysis of **1a** in argon matrices through a Pyrex filter yields **11**; ketene imine formation is a characteristic of the reactivity of triplet vinylnitrenes in matrices.[13,40−42] In contrast, the photolysis of **1b** in argon matrices results in ylide formation, as generally observed for the singlet reactivity of azirines.

3. DISCUSSION

Product studies showed that azirine **1b** does not yield any products when irradiated with light above 300 nm. However, laser flash photolysis and matrix isolation of **1a** with light above 300 nm confirmed the formation of triplet vinylnitrene **5** with a lifetime of 7 μs. The lifetime of vinylnitrene **5** is somewhat
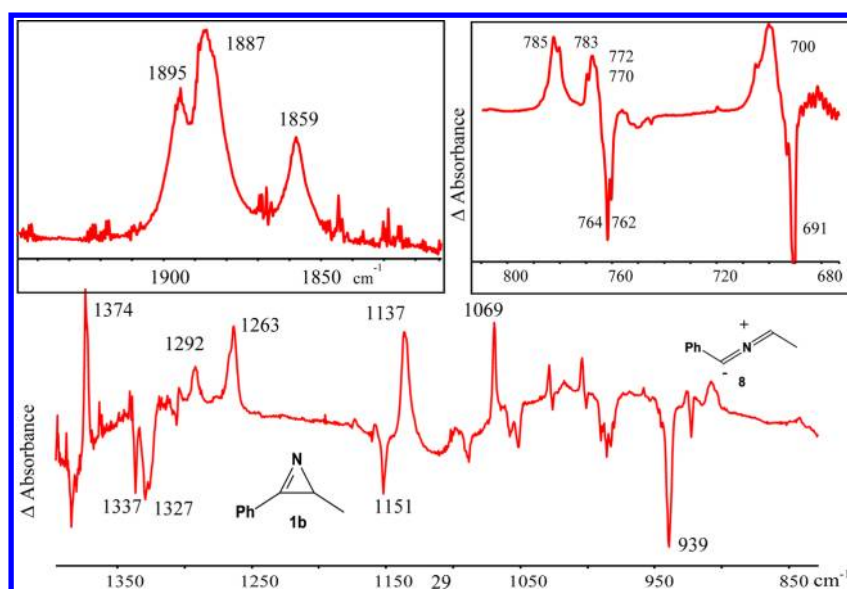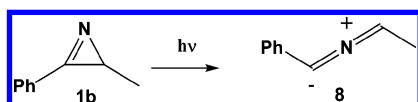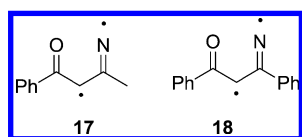
Figure 15. Difference of the IR spectra obtained before and after the irradiation of **1b** through a Pyrex filter. The positive bands belong to **8** and the negative bands to **1b**.

Scheme 8

longer than we previously reported for vinylnitrenes **17** and **18** (depicted in Scheme 9).[11,13]

Scheme 9

We theorize that the greater spin delocalization of **5** stabilizes it more than vinylnitrenes **17** and **18**. The rate constant for interception of vinylnitrene **5** with oxygen is $8.9 \times 10^8 \ M^{-1} \ s^{-1}$, whereas that for trapping of vinylnitrene **5** with bromoform is significantly lower $(1.7 \times 10^5 \ M^{-1} \ s^{-1})$. The lower rate for the reaction of vinylnitrene **5** with bromoform can be a reflection of the larger transition state barrier for the reaction of **5** with bromoform compared with oxygen. However, since direct photolysis of bromoform yields bromine radicals, it is just as likely that the lower rate for the reaction of vinylnitrene **5** with bromoform is a reflection of the fact that the Stern−Volmer plot was graphed using the concentration of bromoform rather than bromine radicals and that a larger rate for the trapping of vinylnitrene **5** would be obtained as a function of bromine radicals.

In comparison, the irradiation of azirine **1b** solely yields ylide **8**, as the formation of vinylnitrene **10** in solution or ketene imine **12** in matrixes was not observed. Thus, when **1b** is irradiated, it forms the S_1 of **1b**, which presumably undergoes internal conversion to a vibrationally hot ground state to overcome the energy barrier of the transition state to form ylide **8** (43 kcal/mol). Because the azirine moiety is in conjugation with the benzene ring, selective excitation of only the phenyl moiety is not possible. In addition, intersystem crossing in **1b** must be slower than in **1a**, as it does not compete with the ylide formation. The intersystem crossing in **1b** is presumably slow because the azirine and phenyl moieties are fully conjugated and thus in more rigid alignment than in **1a**, where the azirine and phenyl π system are orthogonal to each other. Finally, because of the conjugation of the phenyl ring with the azirine moiety in **1b**, the transition state barrier for breaking the C−N bond to form vinylnitrene **10** is considerably larger than that for formaton of vinylnitrene **5** from **1a**.

4. CONCLUSION

We have shown that the photolysis of azirine **1a** through a Pyrex filter results in triplet vinylnitrene formation, whereas irradiation of **1b** yields only ylide formation. The triplet vinylnitrene **5** has a lifetime of a few microseconds and can be trapped both with oxygen and bromine radicals.

5. EXPERIMENTAL SECTION

5.1. Molecular Modeling. All of the geometries were optimized at the B3LYP level of theory with the 6-31G+(d) basis set as implemented in Gaussian09. Transition states were confirmed to have one imaginary vibrational frequency by analytical determination of the second derivatives of the energy with respect to internal coordinates. Intrinsic reaction coordinate (IRC) calculations were used to verify that each located transition state corresponded to the attributed reactant and product.[43,44] The absorption spectra were calculated using time-dependent density functional theory (TD-DFT).[45−47] The effect of solvation was calculated using the self-consistent reaction field (SCRF) method with the integral equation formalism polarization continuum model (IEFPCM) with acetonitrile, methanol, and dichloromethane as solvents.[48−51]

5.2. Laser Flash Photolysis. Laser flash photolysis was performed with an excimer laser (308 nm, 17 ns). The system has been described in detail elsewhere.[52] In a typical experiment, a stock solution of **1a** or **1b** was prepared with spectroscopic-grade acetonitrile such that the solutions had an absorbance between 0.3 and 0.6 at 308 nm. Typically, ∼1 mL of the stock solution was placed in a 10 mm × 10 mm × 48 mm quartz cuvette and purged with argon or oxygen for 5 min. The rate was obtained by fitting the average of two to three kinetic traces.

5.3. Matrix Isolation. Matrix isolation studies were performed using conventional equipment.[53]

5.4. Preparation of Azirines 1a and 1b. *Synthesis of (2-Azido-1-iodopropyl)benzene.* (2-Azido-1-iodopropyl)benzene was prepared following the procedure reported by Nair et al.[54] To a mixture of *trans*-propenylbenzene (2.0 g, 16.9 mmol), sodium azide (1.10 g, 16.9 mmol), and sodium iodide (2.50 g, 16.9 mmol) in methanol (25 mL) at 0 °C was added a solution of ceric ammonium nitrate (19.5 g, 35.6 mmol) in methanol (100 mL) dropwise. When TLC showed that the starting material was exhausted, saturated aqueous NaHSO$_3$ (50 mL) was added, and the resulting mixture was extracted with dichloromethane (3 × 125 mL). The combined organic extracts were washed with distilled water (50 mL) and saturated brine (50 mL) and dried over anhydrous MgSO$_4$, and the solvent was removed under vacuum. The residue was purified on a silica column with hexane and ethyl acetate (9:1) as an eluent to yield (2-azido-1-iodopropyl)benzene (2.3 g, 7.9 mmol, 47% yield) as a slightly yellowish oil.

IR (CDCl$_3$): 2984, 2099, 1451, 1259 cm^{-1}. ^{1}H NMR (CDCl$_3$, 400 MHz): δ 1.25−1.27 (d, *J* = 8 Hz, 3H), 1.54−1.55 (d, *J* = 4 Hz, 3H), 3.81−3.88 (m, 1H), 3.93−4.00 (m, 1H), 4.95−4.97 (d, *J* = 8 Hz, 1H), 5.00−5.02 (d, *J* = 8 Hz, 1H), 7.29−7.50 (m, 10H). ^{13}C NMR (CDCl$_3$, 100 MHz): δ 140.7, 140.4, 128.9, 128.7, 128.5, 128.4, 128.1, 63.7, 63.2, 37.4, 36.3, 19.8, 18.4. GC/MS (EI): *m/z* 217, 127, 117, 105, 91 (100), 77, 65.

Synthesis of (2-Azidoprop-1-en-1-yl)benzene. To 2.3 g (7.9 mmol) of (2-azido-1-iodopropyl)benzene in dry diethyl ether (100 mL) in an ice bath was added potassium *tert*-butoxide (1.2 g, 10.3 mmol). The reaction mixture was stirred for 4 h at 0 °C and was then washed twice with water (100 mL). The organic extract was dried over magnesium sulfate, and the diethyl ether was removed under vacuum at ambient temperature. The residue was subjected to chromatography on silica and eluted with hexane and ethyl acetate (9:1) to yield (*Z*)-(2-azidoprop-1-en-1-yl)benzene (0.91 g, 5.7 mmol, 70% yield) as a colorless oil and (*E*)-(2-azidoprop-1-enyl)benzene (0.13 g, 0.8 mmol, 10% yield) as a colorless oil. The spectra of (2-azidoprop-1-en-yl)benzene are in agreement with those already published.[55]

IR (CDCl$_3$): 2121, 2099, 2055, 1646, 1597, 1572, 1492, 1265 cm^{-1}. ^{1}H NMR (CDCl$_3$, 400 MHz): (*Z* isomer) δ 2.20 (s, 3H), 5.62 (br s, 1H), 7.56−7.15 (m, 5H); (*E* isomer) δ 2.06 (s, 3H), 6.18 (br s, 1H), 7.35−7.17 (m, 5H). ^{13}C NMR (CDCl$_3$, 100 MHz): (*Z* isomer) δ 135.3, 131.1, 128.5, 128.2, 126.6, 115.7, 19.8; (*E* isomer) δ 136.1, 135.4, 128.6, 128.4, 126.6, 115.9, 15.6.

Synthesis of (1-Azido-2-iodopropyl)benzene. Sodium azide (3.58 g, 22 mmol) in acetonitrile (50 mL) was placed in a 100 mL three-neck round-bottom flask fitted with two 50 mL pressure-equalizing dropping funnels. The flask was cooled in an ice bath, and iodine monochloride (2.75 g, 42.4 mmol) was added dropwise from one of the dropping funnels over a period of 15 min while the reaction mixture was stirred with a magnetic stirrer. The solution was stirred for an additional 10 min, and then *trans*-propenylbenzene (2.0 g, 16.9 mmol) was added from the other dropping funnel over a 15 min period. The resulting reaction mixture was stirred for 12 h at ambient temperature, poured into water (50 mL), and extracted with three portions of diethyl ether (50 mL). The combined organic extracts were washed with 5% aqueous sodium thiosulfate (100 mL) and water (100 mL). The ether extract was dried over magnesium sulfate, and the solvent was removed under vacuum at ambient temperature to yield the product as a pale-yellow oil (4.5 g) of sufficient purity to be used for the next step.

IR (CDCl$_3$): 2983, 2099, 1492, 1451, 1259, 752, 700 cm^{-1}. ^{1}H NMR (CDCl$_3$, 400 MHz): δ 1.87−1.88 (d, *J* = 4 Hz, 3H), 4.31−4.38 (m, 1H), 4.75−4.77 (d, *J* = 8 Hz, 1H), 7.32−7.43 (m, 5H). ^{13}C NMR (CDCl$_3$, 100 MHz): δ 137.4, 128.82, 128.75, 127.4, 72.7, 28.8, 23.5. GC/MS (EI): *m/z* 287, 245, 155 (100), 127, 117, 105, 91, 77, 65.

Synthesis of (1-Azidoprop-1-en-1-yl)benzene. (1-Azidoprop-1-en-1-yl)benzene was synthesized following the procedure of Hassner and Fowler.[56] A solution of (1-azido-2-iodopropyl)benzene (4.5 g, 15.7 mmol) in dry diethyl ether (100 mL) was cooled in an ice bath, and to it was added potassium *tert*-butoxide (2.3 g, 20.4 mmol). The reaction was stirred for 4 h at 0 °C and washed with two portions of water (100 mL). The organic layer was dried over magnesium sulfate, and the solvent was removed under vacuum at ambient temperature. The

residue was subjected to silica gel chromatography and eluted with hexane and ethyl acetate (92:8) to yield (1-azidoprop-1-en-1-yl)benzene as a pale-yellow oil (1.79 g, 11.3 mmol, 72% yield).

IR (CDCl$_3$): 2104, 1652, 1492, 1443, 1265, 763, 700 cm^{-1}. ^{1}H NMR (CDCl$_3$, 400 MHz): δ 1.71−1.72 (d, *J* = 4 Hz, 3H), 5.45−5.51 (q, *J* = 8 Hz, 1H), 7.31−7.43 (m, 5H). ^{13}C NMR (CDCl$_3$, 100 MHz): δ 137.3, 133.2, 128.8, 128.6, 128.4, 112.1, 13.8. GC/MS (EI): *m/z* 131 (M$^+$ − N$_2$), 130, 104, 103 (100), 76, 64.

Photolysis of (2-Azidoprop-1-en-1-yl)benzene To Give 1a. A solution of (*Z*)-(2-azidoprop-1-en-1-yl)benzene (450 mg, 2.2 mmol) in chloroform (100 mL) was purged with argon for 15 min and irradiated using a high-pressure mercury lamp through a Pyrex filter (>310 nm) for 8 h. The solvent was removed under vacuum to obtain 1a as a dark-brown oil (359 mg, 2.1 mmol, 97% yield). The spectroscopic characterization of 1a matched the previously published data.[55,57]

IR (CDCl$_3$): 3029, 1764, 1668, 1598, 1495, 1454, 1261, 913, 766 cm^{-1}. ^{1}H NMR (CDCl$_3$, 400 MHz): δ 2.52 (s, 3H), 2.89 (s, 1H), 7.05−7.07 (d, *J* = 8 Hz, 2H), 7.21−7.31 (m, 3H). ^{13}C NMR (CDCl$_3$, 100 MHz): δ 164.5, 141.2, 128.3, 126.8, 125.6, 33.4, 12.9. GC/MS (EI): *m/z* 131, 130 (100), 90, 89, 77, 65.

Photolysis of (1-Azidoprop-1-en-1-yl)benzene To Give 1b. A solution of (1-azidoprop-1-en-1-yl)benzene (300 mg, 1.88 mmol) in chloroform (60 mL) was purged with argon for 15 min and irradiated using a high-pressure mercury lamp through a Pyrex filter (>310 nm) for 10 h. GC/MS analysis of the reaction mixture showed some remaining (1-azidoprop-1-enyl)benzene (5%) and the formation of 1b. The solvent was removed under vacuum, and the resulting oil was purified on a silica column with 10% ethyl acetate in hexane to obtain 1b as a pale-yellow oil (222 mg, 1.70 mmol, 90% yield). The spectra of 1b are in agreement with those already published.[55]

IR (CDCl$_3$): 1737, 1597, 1578, 1487, 1451, 1320, 936, 760, 689 cm^{-1}. ^{1}H NMR (CDCl$_3$, 400 MHz): δ 1.36−1.37 (d, *J* = 4 Hz, 3H), 2.29−2.33 (q, *J* = 4 Hz, 1H), 7.54−7.57 (m, 3H), 7.85−7.87 (m, 2H). ^{13}C NMR (CDCl$_3$, 100 MHz): δ 172.5, 132.7, 129.3, 129.1, 125.7, 27.5, 18.9. GC/MS (EI): *m/z* 131, 130, 104, 103 (100), 77, 76.

5.5. Photolysis of Azirines 1a and 1b. *Photolysis of 1a in Argon-Saturated Acetonitrile.* Azirine 1a (100 mg, 0.76 mmol) was dissolved in acetonitrile, and argon was bubbled through the solution for 15 min. The solution was irradiated using a high-pressure mercury lamp through a Pyrex filter (>310 nm) for 20 h. GC/MS analysis of the irradiated solution showed no new products.

Photolysis of 1a in Oxygen-Saturated Acetonitrile. Azirine 1a (100 mg, 0.76 mmol) was dissolved in acetonitrile, and oxygen was bubbled through the solution for 15 min. The solution was irradiated using a high-pressure mercury lamp through a Pyrex filter (>310 nm) for 20 h. The ^{1}H NMR spectra of the reaction mixture showed the formation of benzaldehyde (2) (11% yield) as the major product along with remaining starting material.

Photolysis of 1a in Argon-Saturated Bromoform. Azirine 1a (100 mg, 0.76 mmol) was dissolved in bromoform, and argon was bubbled through the solution for 15 min. The solution was irradiated using a high-pressure mercury lamp through a Pyrex filter (>310 nm) for 6 h. GC/MS analysis of the reaction mixture showed trace amounts of 1-phenylpropan-2-one (3) and 1-bromo-1-phenylpropan-2-one (4) (14%). The formation of 3 and 4 was verified by injecting authentic samples into the GC/MS instrument.

Photolysis of 1a in Oxygen-Saturated Bromoform. Azirine 1a (100 mg, 0.76 mmol) was dissolved in bromoform, and oxygen was bubbled through the solution for 15 min. The solution was irradiated using a high-pressure mercury lamp through a Pyrex filter (>310 nm) for 15 h. GC/MS analysis of the reaction mixture showed the formation of 2 (10%), 3 (9%), and 4 (81%).

Photolysis of 1b in Argon-Saturated Acetonitrile. Azirine 1b (100 mg, 0.76 mmol) was dissolved in acetonitrile, and argon was bubbled through the solution for 15 min. The solution was irradiated using a high-pressure mercury lamp through a Pyrex filter (>310 nm) for 6 h. The solvent was then removed under vacuum to yield a crude oil. ^{1}H NMR spectroscopy of the reaction mixture showed two significant components, which were assigned as *exo*-2,6-dimethyl-4,5-diphenyl-

1,3-diazabicyclo[3.1.0]hex-3-ene (**6**) and *endo*-2,6-dimethyl-4,5-diphenyl-l,3-diazabicyclo-[3.1.0]hex-3-ene (**7**) on the basis of their ^{1}H NMR spectra, which matched those reported previously.[27]

6: ^{1}H NMR (CDCl$_3$, 400 MHz): δ 1.25 (d, J = 4 Hz, 3H), 1.48−1.50 (d, J = 8 Hz, 3H), 2.04−2.08 (q, J = 4 Hz, 1H), 5.59−5.64 (q, J = 8 Hz, 1H), 7.30−7.50 (m, 10H). **7**: ^{1}H NMR (CDCl$_3$, 400 MHz): δ 1.24 (d, J = 4 Hz, 3H), 1.52 (d, J = 8 Hz, 3H), 2.07 (q, J = 4 Hz, 1H), 5.0 (q, J = 8 Hz, 1H), 7.30−7.50 (m, 10H).

Photolysis of 1b in Oxygen-Saturated Acetonitrile. Azirine **1b** (100 mg, 0.76 mmol) was dissolved in acetonitrile, and oxygen was bubbled through the solution for 15 min. The solution was irradiated using a high-pressure mercury lamp through a Pyrex filter (>310 nm) for 6 h. The solvent was then removed under vacuum to yield a crude oil. ^{1}H NMR spectroscopy showed two products, which were identified as **6** and **7**.

Photolysis of 1b in CO$_2$-Saturated Acetonitrile. Azirine **1b** (100 mg, 0.76 mmol) was dissolved in acetonitrile. CO$_2$ was bubbled through the solution while it was irradiated using a high-pressure mercury lamp through a Pyrex filter (>310 nm) for 4 h. GC/MS was used to monitor the reaction progress. When GC/MS showed that the starting material was depleted, the solvent was removed under vacuum to produce 2-methyl-4-phenyloxazol-5(2*H*)-one (**9**) in 95% yield. The spectroscopic characterization matched the published data.[28]

IR (CDCl$_3$): 2985, 1179, 1618, 1302, 1149, 1066, 928, 808, 747, 686 cm^{-1}. ^{1}H NMR (CDCl$_3$, 400 MHz): δ 1.66−1.68 (d, J = 8 Hz, 3H), 6.10−6.15 (q, J = 8 Hz, 1H), 7.48−7.57 (m, 3H), 8.37−8.39 (d, J = 8 Hz, 2H).

■ ASSOCIATED CONTENT

Ⓢ Supporting Information

Cartesian coordinates and energies of **1a**, **1b**, **5**, **8**, and **10−16** and ^{1}H and ^{13}C NMR spectra of **1a**, **1b**, **2**, **3**, **4**, **6**, **7**, and **9**. This material is available free of charge via the Internet at http://pubs.acs.org.

■ AUTHOR INFORMATION

Corresponding Author

*E-mail: Anna.Gudmundsdottir@uc.edu.

Notes

The authors declare no competing financial interest.

■ ACKNOWLEDGMENTS

■ REFERENCES

(1) Platz, M. S. Nitrenes. In *Reactive Intermediate Chemistry*; Moss, R. A., Platz, M. S., Jones, M., Jr., Eds.; John Wiley & Sons: Hoboken, NJ, 2004; Chapter 11.

(2) Reiser, A.; Leyshon, L. J. *J. Am. Chem. Soc.* **1971**, *93*, 4051.

(3) Schrock, A. K.; Schuster, G. B. *J. Am. Chem. Soc.* **1984**, *106*, 5228.

(4) Muthukrishnan, S.; Ranaweera, R. A. A. U.; Gudmundsdottir, A. D. In *Nitrenes and Nitrenium Ions*; Falvey, D. E., Gudmundsdottir, A. D., Eds.; John Wiley & Sons: Hoboken, NJ, 2013; Vol. 6.

(5) Singh, P. N. D.; Mandel, S. M.; Sankaranarayanan, J.; Muthukrishnan, S.; Chang, M.; Robinson, R. M.; Lahti, P. M.; Ault, B. S.; Gudmundsdottir, A. D. *J. Am. Chem. Soc.* **2007**, *129*, 16263.

(6) Sankaranarayanan, J.; Bort, L. N.; Mandel, S. M.; Chen, P.; Krause, J. A.; Brooks, E. E.; Tsang, P.; Gudmundsdottir, A. D. *Org. Lett.* **2008**, *10*, 937.

(7) Sankaranarayanan, J.; Rajam, S.; Hadad, C. M.; Gudmundsdottir, A. D. *J. Phys. Org. Chem.* **2010**, *23*, 370.

(8) Lwowski, W.; Woerner, F. P. *J. Am. Chem. Soc.* **1965**, *87*, 5491.

(9) Lwowski, W.; Mattingly, T. W., Jr. *J. Am. Chem. Soc.* **1965**, *87*, 1947.

(10) Murthy, R. S.; Muthukrishnan, S.; Rajam, S.; Mandel, S. M.; Ault, B. S.; Gudmundsdottir, A. D. *J. Photochem. Photobiol., A* **2009**, *201*, 157.

(11) Gamage, D. W.; Li, Q.; Ranaweera, R. A. A. U.; Sarkar, S. K.; Weragoda, G. K.; Carr, P. L.; Gudmundsdottir, A. D. *J. Org. Chem.* **2013**, *78*, 11349.

(12) Nunes, C. M.; Reva, I.; Pinho e Melo, T. M. V. D.; Fausto, R.; Šolomek, T.; Bally, T. *J. Am. Chem. Soc.* **2011**, *133*, 18911.

(13) Rajam, S.; Murthy, R. S.; Jadhav, A. V.; Li, Q.; Keller, C.; Carra, C.; Pace, T. C. S.; Bohne, C.; Ault, B. S.; Gudmundsdottir, A. D. *J. Org. Chem.* **2011**, *76*, 9934.

(14) Singh, B.; Zweig, A.; Gallivan, J. B. *J. Am. Chem. Soc.* **1972**, *94*, 1199.

(15) Inui, H.; Murata, S. *J. Am. Chem. Soc.* **2005**, *127*, 2628.

(16) Murata, S.; Tomioka, H. *Chem. Lett.* **1992**, 57.

(17) Nunes, C. M.; Reva, I.; Fausto, R. *J. Org. Chem.* **2013**, *78*, 10657.

(18) Gritsan, N. P.; Pritchina, E. S. *J. Inf. Rec. Mater.* **1989**, *17*, 391.

(19) Pritchina, E. A.; Gritsan, N. P. *J. Photochem. Photobiol., A* **1988**, *43*, 165.

(20) Barcus, R. L.; Hadel, L. M.; Johnston, L. J.; Platz, M. S.; Savino, T. G.; Scaiano, J. C. *J. Am. Chem. Soc.* **1986**, *108*, 3928.

(21) Mueller, F.; Mattay, J. *Chem. Ber.* **1993**, *126*, 543.

(22) Orton, E.; Collins, S. T.; Pimentel, G. C. *J. Phys. Chem.* **1986**, *90*, 6139.

(23) Albrecht, E.; Mattay, J.; Steenken, S. *J. Am. Chem. Soc.* **1997**, *119*, 11605.

(24) Gakis, N.; Maerky, M.; Hansen, H. J.; Schmid, H. *Helv. Chim. Acta* **1972**, *55*, 748.

(25) Bayes, K. D.; Toohey, D. W.; Friedl, R. R.; Sander, S. P. *J. Geophys. Res.: Atmos.* **2003**, *108*, ACH4/1.

(26) Padwa, A.; Smolanoff, J.; Wetmore, S. I., Jr. *J. Chem. Soc., Chem. Commun.* **1972**, 409.

(27) Padwa, A.; Smolanoff, J.; Wetmore, S. I., Jr. *J. Org. Chem.* **1973**, *38*, 1333.

(28) Padwa, A.; Akiba, M.; Cohen, L. A.; MacDonald, J. G. *J. Org. Chem.* **1983**, *48*, 695.

(29) Jackson, B.; Gakis, N.; Märky, M.; Hansen, H. J.; von Philipsborn, W.; Schmid, H. *Helv. Chim. Acta* **1972**, *55*, 916.

(30) Padwa, A.; Wetmore, S. I. *J. Am. Chem. Soc.* **1974**, *96*, 2414.

(31) Frisch, M. J.; Trucks, G. W.; Schlegel, H. B.; Scuseria, G. E.; Robb, M. A.; Cheeseman, J. R.; Scalmani, G.; Barone, V.; Mennucci, B.; Petersson, G. A.; Nakatsuji, H.; Caricato, M.; Li, X.; Hratchian, H. P.; Izmaylov, A. F.; Bloino, J.; Zheng, G.; Sonnenberg, J. L.; Hada, M.; Ehara, M.; Toyota, K.; Fukuda, R.; Hasegawa, J.; Ishida, M.; Nakajima, T.; Honda, Y.; Kitao, O.; Nakai, H.; Vreven, T.; Montgomery, J. A., Jr.; Peralta, J. E.; Ogliaro, F.; Bearpark, M.; Heyd, J. J.; Brothers, E.; Kudin, K. N.; Staroverov, V. N.; Kobayashi, R.; Normand, J.; Raghavachari, K.; Rendell, A.; Burant, J. C.; Iyengar, S. S.; Tomasi, J.; Cossi, M.; Rega, N.; Millam, J. M.; Klene, M.; Knox, J. E.; Cross, J. B.; Bakken, V.; Adamo, C.; Jaramillo, J.; Gomperts, R.; Stratmann, R. E.; Yazyev, O.; Austin, A. J.; Cammi, R.; Pomelli, C.; Ochterski, J. W.; Martin, R. L.; Morokuma, K.; Zakrzewski, V. G.; Voth, G. A.; Salvador, P.; Dannenberg, J. J.; Dapprich, S.; Daniels, A. D.; Farkas, Ö.; Foresman, J. B.; Ortiz, J. V.; Cioslowski, J.; Fox, D. J. *Gaussian 09*, revision A.1; Gaussian, Inc.: Wallingford, CT, 2009.

(32) Becke, A. D. *J. Chem. Phys.* **1993**, *98*, 5648.

(33) Lee, C.; Yang, W.; Parr, R. G. *Phys. Rev. B* **1988**, *37*, 785.

(34) Muthukrishnan, S.; Mandel, S. M.; Hackett, J. C.; Singh, P. N. D.; Hadad, C. M.; Krause, J. A.; Gudmundsdottir, A. D. *J. Org. Chem.* **2007**, *72*, 2757.

(35) Parasuk, V.; Cramer, C. J. *Chem. Phys. Lett.* **1996**, *260*, 7.

(36) Wenthold, P. G. *J. Org. Chem.* **2012**, *77*, 208.

(37) Hossain, E.; Wenthold, P. G. *Comput. Theor. Chem.* **2013**, *1020*, 180.

(38) Clark, W. D. K.; Steel, C. *J. Am. Chem. Soc.* **1971**, *93*, 6347.

(39) Foresman, J. B.; Frisch, Æ. *Exploring Chemistry with Electronic Structure Methods*, 2nd ed.; Gaussian, Inc.: Pittsburgh, PA, 1996.

(40) Inui, H.; Murata, S. *Chem. Lett.* **2001**, *30*, 832.

(41) Kaczor, A.; Gómez-Zavaglia, A.; Cardoso, A. L.; Pinho e Melo, T. M. V. D.; Fausto, R. *J. Phys. Chem. A* **2006**, *110*, 10742.

(42) Inui, H.; Murata, S. *Chem. Commun.* **2001**, 1036.

(43) Gonzalez, C.; Schlegel, H. B. *J. Chem. Phys.* **1989**, *90*, 2154.

(44) Gonzalez, C.; Schlegel, H. B. *J. Phys. Chem.* **1990**, *94*, 5523.

(45) Bauernschmitt, R.; Ahlrichs, R. *Chem. Phys. Lett.* **1996**, *256*, 454.

(46) Stratmann, R. E.; Scuseria, G. E.; Frisch, M. J. *J. Chem. Phys.* **1998**, *109*, 8218.

(47) Foresman, J. B.; Head-Gordon, M.; Pople, J. A.; Frisch, M. J. *J. Phys. Chem.* **1992**, *96*, 135.

(48) Cances, E.; Mennucci, B. *J. Chem. Phys.* **2001**, *114*, 4744.

(49) Cramer, C. J.; Truhlar, D. G. *Chem. Rev.* **1999**, *99*, 2161.

(50) Mennucci, B.; Cances, E.; Tomasi, J. *J. Phys. Chem. B* **1997**, *101*, 10506.

(51) Tomasi, J.; Mennucci, B.; Cammi, R. *Chem. Rev.* **2005**, *105*, 2999.

(52) Muthukrishnan, S.; Sankaranarayanan, J.; Klima, R. F.; Pace, T. C. S.; Bohne, C.; Gudmundsdottir, A. D. *Org. Lett.* **2009**, *11*, 2345.

(53) Ault, B. S. *J. Am. Chem. Soc.* **1978**, *100*, 2426.

(54) Nair, V.; George, T. G.; Sheeba, V.; Augustine, A.; Balagopal, L.; Nair, L. G. *Synlett* **2000**, 1597.

(55) Bader, H.; Hansen, H. J. *Helv. Chim. Acta* **1978**, *61*, 286.

(56) Hassner, A.; Fowler, F. W. *Tetrahedron Lett.* **1967**, *8*, 1545.

(57) Singh, P. N. D.; Carter, C. L.; Gudmundsdottir, A. D. *Tetrahedron Lett.* **2003**, *44*, 6763.